



Slight flow volume rises increase nitrogen loading to nitrogen-rich river, while dramatic flow volume rises promote nitrogen consumption



Jiali Lü^{a,b,c,e}, Shiqin Wang^{a,d,*}, Binbin Liu^{a,d}, Wenbo Zheng^a, Kangda Tan^a, Xianfang Song^{b,c,e}

^a Key Laboratory of Agricultural Water Resources, Center for Agricultural Resources Research, Institute of Genetics and Developmental Biology, Chinese Academy of Sciences, Shijiazhuang 050021, China

^b Sino-Danish College of University of Chinese Academy of Sciences, Beijing 101408, China

^c Sino-Danish Centre for Education and Research, Beijing 101408, China

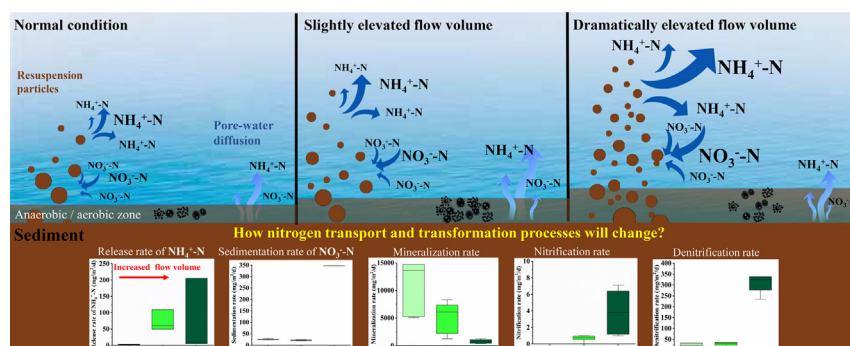
^d Xiongan Institute of Innovation, Chinese Academy of Science, China

^e Key Laboratory of Water Cycle & Related Land Surface Processes, Institute of Geographic Sciences and Natural Resources Research, Chinese Academy of Sciences, Beijing 100101, China

HIGHLIGHTS

- A model was developed to simulate nitrogen transport and transformation processes.
- The slight increase in flow volume increases inorganic N loading in river.
- Dramatic elevated flow volume promotes inorganic N consumption.
- High flow volume may enhance the role of microbial N-related functional gene.

GRAPHICAL ABSTRACT



ARTICLE INFO

Editor: José Virgílio Cruz

Keywords:

Nitrogen exchange flux
Nitrogen transport
Resuspension
Functional gene composition
Water diversion

ABSTRACT

Concentrated rainfall and water transfer projects result in slight and dramatic increases in flow volume over short periods of time, causing nitrogen recontamination in the water-receiving areas of nitrogen-rich rivers. This study coupled hydrodynamic and biochemical reaction models to construct a model for quantifying diffusive transport and transformation fluxes of nitrogen across the water-sediment interface and analysed possible changes in the relative abundance of microbial functional genes using high-throughput sequencing techniques. In this study, the processes of ammonium (NH_4^+-N) and nitrate (NO_3^--N) nitrogen release and sedimentation with resuspended particles, as well as mineralisation, nitrification, and denitrification processes were investigated at the water-sediment interface in the Fu River during slight and dramatic increases in flow volume caused by concentrated rainfall and water diversion projects. Specifically, a slight flow volume rise increased the release of NH_4^+-N from the sediment, inhibited sedimentation of NO_3^--N , decreased the mineralisation rate, increased the nitrification rate, and had little effect on the denitrification process, ultimately increasing the nitrogen load to the river water. A dramatic increase in flow volume simultaneously increased NH_4^+-N and NO_3^--N exchange fluxes, inhibited the mineralisation process, promoted nitrification-denitrification processes, and increased inorganic nitrogen consumption in the river. This study provides a solution for the re-pollution of rivers that occurs during the implementation of reservoir management and water diversion projects. Furthermore, these results indicate a potential global nitrogen sink that may have been overlooked.

* Corresponding author at: Key Laboratory of Agricultural Water Resources, Center for Agricultural Resources Research, Institute of Genetics and Developmental Biology, Chinese Academy of Sciences, Shijiazhuang 050021, China.

E-mail address: sqwang@sjziam.ac.cn (S. Wang).

1. Introduction

Although measures to limit external N have been commonly applied to rivers, most of the rivers are still affected by eutrophication (Malone and

Newton, 2020; Rääke et al., 2020). Sediment plays a major role in the transportation and transformation of nutrients in rivers because of its capacity to store and release different compounds in the water (Brigolin et al., 2011; Schacht et al., 2008). The release of N from sediments contributes to instant concentrations of N in eutrophic lakes, accounting for 30–44 % of the total loading (Shayo and Limbu, 2018). Exploring the mechanism of N exchange at the water-sediment interface is important for studying eutrophication in rivers, which is a concern for the global N cycle (Conley et al., 2009; Ferguson et al., 2020).

N exchange between water and sediment shows heterogeneity in time and space, and is affected by water temperature, water depth, pH, dissolved oxygen (DO), and hydrodynamic disturbance (Gao et al., 2021; Zhang et al., 2020). Furthermore, in recent years, the impact of human activities on flow volume of rivers has become more pronounced than that of seasonal changes (Brase et al., 2018; Lv et al., 2021). Large-scale hydraulic projects, such as water diversions and dam construction, are widely carried out worldwide to satisfy water supply in water-deficient areas. However, dramatic increases in flow volumes in water-receiving areas are also accompanied by higher total N loading and poorer water quality (Lv et al., 2021; Tao et al., 2019). This phenomenon is particularly pronounced in nitrogen-rich rivers (Yu and Zhang, 2021). Therefore, to eliminate the negative effects of concentrated rainfall and large man-made hydraulic projects on N loading to rivers, the response of N transport and transformation processes at the water-sediment interface to different variations in flow volume (seasonal variations leading to slight increase in flow volume and water transfers leading to dramatic increase in flow volume) needs to be explored (Wang et al., 2018).

Different patterns of N release and microbial interactions at the water-sediment interface have been observed, with slight and dramatic increases in flow volume (Leu et al., 1996; Mihiranga et al., 2021). Wiegner et al. (2013) found that when the flow volume increased slightly, the total nitrogen (TN) load to the river increased slightly, with dissolved organic N being the predominant component (Hitchcock and Mitrovic, 2013). During extreme rainfall periods with sharp increases in flow volume, TN load to the river increased significantly, with ammonium nitrogen ($\text{NH}_4^+ - \text{N}$) concentration showing a logarithmic relationship with the peak flow rate (Ballantine and Davies-Colley, 2013). Closed interactions between the microbial community at the river water-sediment interface, and particulate organic N and resuspended particles exist during slight increases in flow volume, whereas microbial community activity is associated only with resuspended particles under dramatic increases in flow volume (Yang et al., 2021). However, the processes and mechanisms of N exchange affected by slight or dramatic increases in flow volume at the water-sediment interface are still not fully clear.

It is generally accepted that an increased flow volume could affect the vertical transport flux of N across the water-substrate interface by stimulating resuspension processes (physical processes) and altering the rate of remineralisation, nitrification, and denitrification (biochemical processes) associated with microorganisms (Kuypers et al., 2018; Queste et al., 2016; Reisinger et al., 2016). Both the processes (physical and biochemical) are closely related to the concentration of resuspended particles. Specifically, an elevated flow volume increases the shear stress at the streambed, which greatly increases the concentration of resuspended particles, releasing N from particles initially adsorbed on sediment into water or causing N in the water to adsorb onto the resuspended particles (Wang et al., 2021a, 2021b). Resuspended particles provide a unique habitat for water and sediment microorganisms, and their flux affects the composition and diversity of microbial communities within rivers and further interferes with the N transformation processes in rivers (Harrison et al., 2011; Lin et al., 2020) which directly influences the probability of microbial contact with organic particles and affects the rate of N mineralisation (Karthäuser et al., 2021). Microorganisms with denitrification genes (*nirS*) are more likely to attach to resuspended particles (Tao et al., 2021; Wang et al., 2021a, 2021b). The surface layer of the resuspended particles forms a specific micro-redox transition environment that facilitates the coupled processes of nitrification and denitrification, leading to increased

denitrification efficiency at the water-sediment interface (Xia et al., 2017). Therefore, it is reasonable to infer that both slight and dramatic flow increases have different effects on the resuspension and biochemical processes of the N fluxes.

Numerous methods have been used to model N transport and transformation in rivers. The combination of hydrogen and oxygen isotopes with Bayesian models is the most classical approach to studying riverine N dynamics and can identify N input, transformation, and output processes (Bustillo et al., 2011; Ryu et al., 2021). However, the accuracy of this method is highly dependent on sampling frequency, and it is difficult to achieve N flux predictions for a wide range of scenarios (Ren et al., 2021). Therefore, numerical simulation techniques including LOADEST models (Zhang and Chen, 2014), Monte Carlo methods (Worrall et al., 2012), SWAT models (Ha et al., 2018), and empirical models (Chen et al., 2014; van der Wulp et al., 2016) have been widely used. In these studies, coupled river flow volume, nutrient flux, and nutrient dispersion models were able to identify, to some extent, the main sources of N and the causes of N gradients, and quantify N export fluxes (Alexander et al., 2009). David et al. (2019) argued that the existing N flux models ignore or grossly generalise river resuspension fluxes, leading to biased simulations of N release from river sediments, and highlighted the irreplaceable role of resuspended particles in N transport. Therefore, it is crucial to develop a fully coupled physical-biochemical model that includes resuspension fluxes (Dagg et al., 2007).

In this study, a nitrogen-rich river located in a temperate monsoon zone with regular water diversions was selected to study the physical and biochemical N transport transformation processes at the water-sediment interface. Models considering physical sorption and hydrodynamic and biochemical reaction processes were combined with 16S ribosomal ribonucleic acid (rRNA) high-throughput sequencing techniques to investigate the changes in N transport and transformation processes affected by two different flow increase scenarios: a slight flow volume increase due to concentrated rainfall and a dramatic flow volume increase due to a water transfer project. The objectives of this study were to: 1) develop a method that considers resuspension fluxes to quantify the exchange flux of N at the water-sediment interface; 2) investigate the response of N transport and transformation processes (physical and biochemical processes) to flow volume variability at the water-sediment interface; and 3) determine their relationship to changes in the microbial communities in water and sediment. This study can provide theoretical support for coping with the degradation of the river water quality due to large water transfer projects and dam construction, providing new ideas to alleviate high N loading to the water environment.

2. Materials and methods

2.1. Study area and sampling

The study area, along the course of the Fu River, spans from east of Baoding City to the estuary of Baiyangdian Lake (38°48′–38°55′ N, 115°34′–115°91′ E; Fig. 1). Baiyangdian Lake is the largest freshwater lake on the North China Plain and the core waters of the Xiong'an New Area, a new national zone in China. Among the eight rivers that flow into Lake Baiyangdian, the only perennial one is the Fu River, which is mainly polluted by municipal sewage (with or without primary treatment) from Baoding City (Zhu et al., 2019). This has resulted in a TN content of 1000–3000 mg/kg in the sediment. The study area has a temperate monsoon climate and a concentrated rainfall period. The average annual temperature is approximately 7 °C, with an average of –9 °C in January and 21 °C in June. The annual rainfall was 615.7 mm in 2020, of which approximately 60 % occurred between July and September. August is usually the month with concentrated rainfall (Fig. 2). The annual runoff of the Fu River is 1.83 billion m^3/a . It has been receiving at least 100 million m^3/a of Yellow River water from every December to February since 2018. The water transferred to the river increased to 4.3 billion m^3/a in 2020, causing a considerable impact on its hydrodynamic conditions.

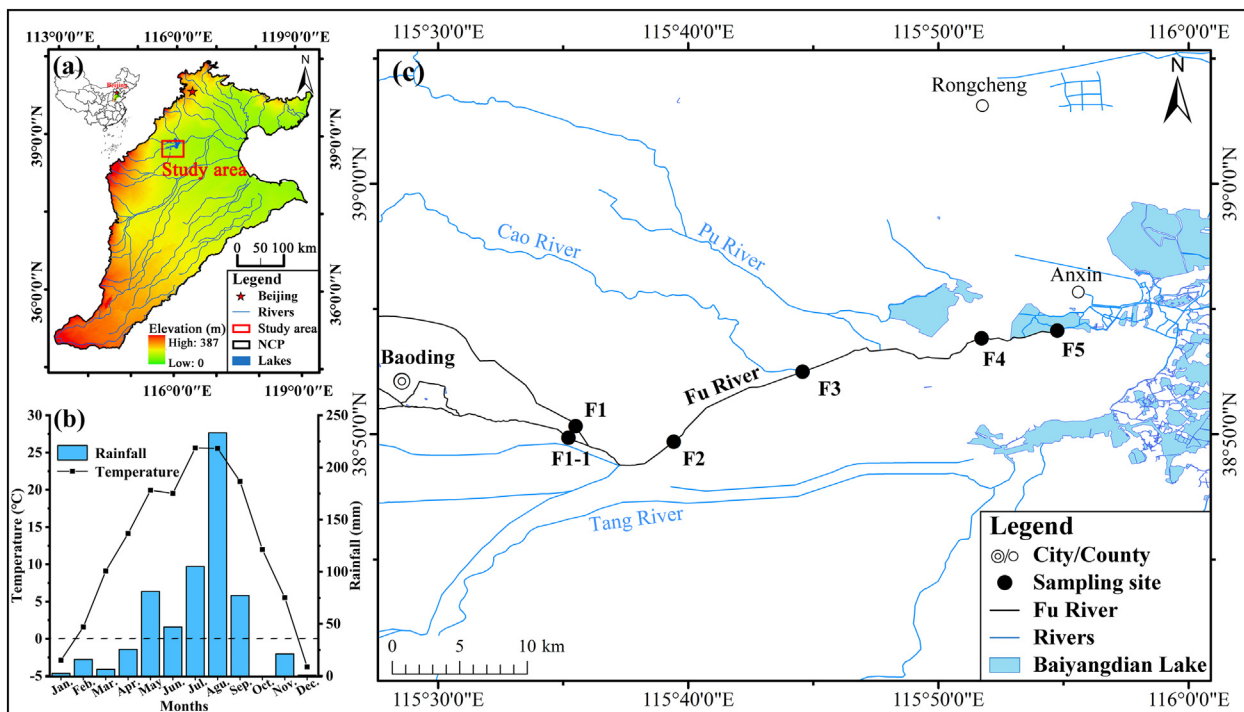


Fig. 1. The study area is located in the North China Plain (NCP, a), with evident seasonal variations in temperature and precipitation in 2020 (Data from National Meteorological Science Data Centre of China, b). Seven sampling sites located along the course of Fu River (c).

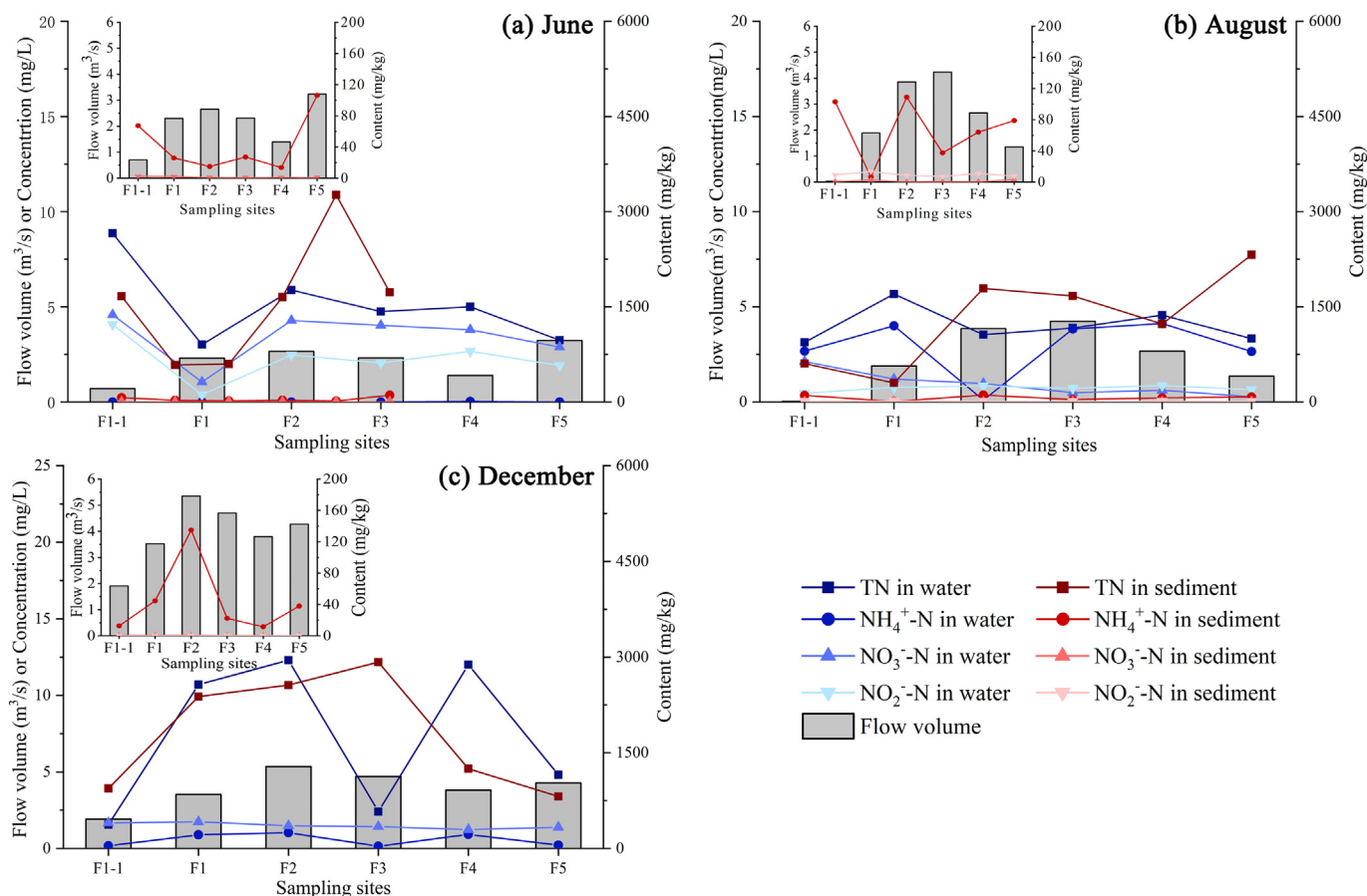


Fig. 2. Nitrogen concentrations in water and sediment and flow volume along Fu River before (June, a) and during concentrated rainfall (August, b), and water diversion period (December, c). The mini-plot shows flow volume and levels of $\text{NH}_4^+\text{-N}$, $\text{NO}_3\text{-N}$, and $\text{NO}_2\text{-N}$ in sediment.

2.2. Data collection

Water and sediment samples were collected from the six sampling sites, of which the sites F1 and F1-1 were located approximately 3 km downstream of the mainstem and tributaries flowing through Baoding City (Fig. 1). F2 was located 3.8 km downstream of the tributary confluence and was the first section to monitor the main stream of the Fu River. F5 was located approximately 3.3 km upstream from the Fu River inlet to Baiyangdian Lake. F3 and F4 were evenly distributed between F2 and F5.

Sample collection and in-situ measurements were conducted three times on 25th June, 24th August, and 17th December 2020, representing the time before and during the summer rainy season, and the winter water transfer period, respectively. Before sampling, physicochemical parameters such as water temperature, pH, electrical conductivity, and oxidation-reduction potential were measured using a portable meter (HORIBA U-51, Horiba, KYO, JPN). The flow volume was measured using Doppler flowmetry (River Surveyor-S5/M9, YSI Corporation, OSU, USA). Water samples were collected from depths exceeding 20 cm from the water surface in the centre of the river and loaded into three 500 mL and three 100 mL polyethylene bottles for deoxyribonucleic acid (DNA) extraction and physicochemical analysis for deoxyribonucleic acid (DNA) extraction and physicochemical analysis at $-80\text{ }^{\circ}\text{C}$ and $4\text{ }^{\circ}\text{C}$ respectively.

To avoid sampling from the active aerobic nitrification zone at the water-sediment interface (top few millimetres) and to ensure that the samples represented recent sediment environment, sediment samples were collected from a depth of 1–2 cm. Three samples were collected from each sampling site after homogenising the sediment at the five locations in a $1 \times 1\text{ m}$ area. The samples were sealed in 10 mL aseptic centrifugal tubes for DNA extraction and in sterile zip-lock bags weighing 1 kg for physicochemical analysis (Campos et al., 2021; Gayathri et al., 2021). All sediment samples were frozen on dry ice immediately after collection and stored at $-80\text{ }^{\circ}\text{C}$ until the start of experiments (Yang et al., 2017).

The concentrations of NO_2^- and NO_3^- in the water were determined using ion chromatography (Dionex ICS-900), and the results were verified by anion and charge balance to ensure a credible margin of error within $\pm 5\%$ (Hodgkins et al., 1998). The TN and NH_4^+-N of water were measured using the Kjeldahl method and alkali solution diffusion method, respectively (Singh et al., 2004). TN and NO_2^- -N contents in the sediment were determined using the Kjeldahl method (Stafilov et al., 2020) and potassium chloride solution extraction–spectrophotometric method (Kaveeshwar et al., 1991), respectively. NO_3^- -N and NH_4^+-N contents in the sediment were quantified by flow injection analysis (Hiroshi, 1991). In addition, the organic N content was calculated by subtracting the inorganic N content from the TN content (Czerwionka, 2016). The instruments used included a UV spectrophotometer (SB-823, HACH, COLO, USA), Titrette 50 mL digital titrator (C-20, Brand, BSE, GER) and Continuous Flow Analyzer (AutoAnalyzer 3, Bran + Luebbe, BER, GER). The particle size (PS) of the river sediment samples was analysed using a laser particle size analyzer (Mastersizer 3000).

2.3. Model description

NH_4^+-N and NO_3^- -N are the main inorganic N components in aquatic environments and are important contributors to N pollution (Gao et al., 2019; Lunau et al., 2013). It is generally accepted that molecular diffusion of pore water occurs in static water systems due to concentration gradients and microbially mediated N transformation processes (Müller et al., 2003). In dynamic water systems, there is a logarithmic relationship between the release of TN during resuspension and the flow rate because of the different sorption-desorption characteristics of NH_4^+-N and NO_3^- -N on particulate matter (Wu et al., 2016; Wu et al., 2015). Therefore, it was hypothesised that the transport mechanisms of NH_4^+-N and NO_3^- -N at the river water-sediment interface are molecular diffusion and resuspension processes that coexist and do not interfere with each other, resulting in the physical release or sedimentation of N. These physical processes, together with biochemical processes including mineralisation, nitrification, and

denitrification, constitute the main N transport and transformation processes at the river water-sediment interface. Considering that the Fu River is nitrogen-rich, the levels of NH_4^+-N and NO_3^- -N in the water and sediment were assumed to be sufficient for both physical transport and microbially mediated biochemical processes. Accordingly, the widely used models of physical transport and biochemical reactions of N have been coupled in the form of a direct superposition to construct mechanistic models capable of quantifying N transport and transformation fluxes at the river water-sediment interface (Yu et al., 2017; Zhong et al., 2017). The values of model parameters were shown in Supplementary Table 1.

2.3.1. Nitrogen transport flux at the water-sediment interface

The molecular diffusion of NH_4^+-N and NO_3^- -N was modelled using Fick's first law (Meng et al., 2020; Müller et al., 2003). According to validation of indoor experiments, the sorption and desorption of NH_4^+-N were described using the Langmuir model and mathematical models of primary kinetic reactions, and the sorption and desorption of NO_3^- -N were simulated using quasi-secondary kinetic models (Huang, 2017; Vandenbruwane et al., 2007). The widely accepted Garcia's model (García and Parker, 1993) was used to calculate resuspension flux as sorbent concentration in these models. The adsorption and desorption of NH_4^+-N and NO_3^- -N to the resuspended particles were assumed to occur simultaneously. This study quantified the release fluxes of NH_4^+-N and NO_3^- -N during resuspension using a desorption model minus sorption model. The model parameters were derived from field measurements and empirical values reported in the literature. Therefore, the model describing NH_4^+-N transport fluxes at the water-sediment interface is

$$F_{\text{NH}_4} = \left(q_{\text{max}} \frac{K_L E_s}{1 + K_L E_s} - E_s \times C_{\text{NH}_4} \times K_d \right) + \left(\varphi \times D_s \times \frac{\partial C}{\partial X} \right) \quad (1)$$

$$E_s = \frac{AZ_u^5}{\left(1 + \frac{A}{0.3 Z_u^5} \right)} \quad (2)$$

$$Z_u^5 = \frac{u_*}{w_r} f(Re_p) \quad (3)$$

where F_{NH_4} is the flux of NH_4^+-N transport at the water-sediment interface ($\text{mg}\cdot\text{m}^{-2}\cdot\text{d}^{-1}$), q_{max} is the maximum adsorption capacity of the sediment ($\text{mg}\cdot\text{kg}^{-1}$), K_L is the equilibrium adsorption constant, E_s is the sediment entrainment flux during resuspension ($\text{mg}\cdot\text{m}^{-2}\cdot\text{d}^{-1}$), C_{NH_4} is the concentration of NH_4^+-N in the sediment from field data ($\text{mg}\cdot\text{L}^{-1}$), K_d denotes the desorption equilibrium constant, $\frac{\partial C}{\partial X}$ is the concentration gradient of the material at the water-sediment interface ($\text{mg}\cdot\text{L}^{-1}\cdot\text{cm}^{-1}$), and D_s is the actual molecular diffusion coefficient considering the sediment bending effects ($\text{m}^2\cdot\text{s}^{-1}$). The empirical relationship with porosity is represented as $D_s = \varphi D_0$ ($\varphi < 0.7$); $D_s = \varphi^2 D_0$ ($\varphi > 0.7$), where D_0 is the ideal diffusion coefficient for an infinitely dilute solution ($\text{cm}^2\cdot\text{s}^{-1}$) and φ is the sediment porosity and is calculated using the PS measured in the laboratory. A is an empirical constant equal to 1.3×10^{-7} , u_* denotes the bed shear velocity ($\text{m}\cdot\text{s}^{-1}$), w_r is the gravitational settling speed ($\text{m}\cdot\text{s}^{-1}$). The Reynolds coefficient $Re_p = \frac{\sqrt{gRPS^3}}{\nu}$, where R is the settling specific gravity, PS is the sediment particle size (μm); g is the acceleration of gravity and takes the value of $9.8\text{ m}\cdot\text{s}^{-2}$, and ν is the dynamic viscosity coefficient of the water (Pas).

Based on the results of the indoor experiments, models suitable for the adsorption/desorption processes of NO_3^- -N and NH_4^+-N were different. For NO_3^- -N, the most suitable models for sorption and uptake are the quasi-secondary kinetic model and mathematical model for the primary kinetic reaction, respectively (Huang, 2017). Thus, the transport fluxes of NO_3^- -N at the water-sediment interface are:

$$F_{\text{NO}_3} = E_s \times (q_{\text{es}} - q_{\text{ea}}) + \left(\varphi \times D_s \times \frac{\partial C}{\partial X} \right) \quad (4)$$

$$q_{es} = \left(\frac{H_s}{k_s} \right)^{\frac{1}{2}} \quad (5)$$

$$q_{ea} = \left(\frac{H_a}{k_a} \right)^{\frac{1}{2}} \quad (6)$$

where F_{NO_3} is the flux of NO_3^- -N transport at the water-sediment interface ($mg \cdot m^{-2} \cdot d^{-1}$), q_{es}/q_{ea} denote the equilibrium desorption/adsorption ($mg \cdot kg^{-1}$), H_s/H_a represent the initial desorption/adsorption rate (Huang et al., 2017), k_s/k_a denote the quasi-secondary reaction rate ($kg \cdot mg^{-1} \cdot min^{-1}$).

2.3.2. Mineralisation

The mineralisation model (Chapelle, 1995) was used to quantify organic N in the sediment that was mineralised to NH_4^+ -N by microorganisms. It can simulate rate of mineralisation in sediment, considering sediment mineralisation as a function of temperature and dissolved oxygen (Serpa et al., 2007):

$$N_{min} = minN_s \times e^{(KT \times T)} \times N_{os} \times f(O_2) \quad (7)$$

where N_{min} represents the rate of mineralisation at the water-sediment interface ($mg \cdot L^{-1} \cdot d^{-1}$), $minN_s$ is the benthic mineralisation rate of organic N at 0 °C (d^{-1}), KT is the rate of increase in temperature ($^{\circ}C^{-1}$), T is the temperature ($^{\circ}C$), N_{os} is the organic N concentration of sediment particles ($\mu g \cdot g^{-1} \cdot dw$), and $f(O_2)$ is the oxygen limitation expressed by the Michaelis-Menten equation (Chapelle, 1995) as:

$$f(O_2) = \frac{O_2}{O_2 + K_{min}O_2} \quad (8)$$

where $K_{min}O_2$ is the half-saturation coefficient for mineralisation ($g \cdot m^{-3}$) and O_2 is the DO of water ($mg \cdot L^{-1}$, field data).

2.3.3. Nitrification/denitrification

The nitrification rate is related to oxygen, temperature, and NH_4^+ . These relationships were simulated using the inverse Michaelis-Menten equation (Chapelle, 1995):

$$N_N = k_{NO} \nu_N^{T-20} \left(\frac{O_2}{K_{NIT} + O_2} \right) C_{NH4} \quad (9)$$

where N_N represents the nitrification rate at the water-sediment interface ($mg \cdot L^{-1} \cdot d^{-1}$), C_{NH4} and O_2 are the near-bottom concentrations ($mg \cdot L^{-1}$), k_{NO} is a coefficient that parameterises the effects of a characteristic local nitrification rate and an average rate of diffusion between the sediments and water (d^{-1}), ν_N is the temperature-rate coefficient for nitrification, T is the water temperature from field data ($^{\circ}C$, Table 1), K_{NIT} represents the nitrification half-saturation constant for oxygen ($g \cdot m^{-3}$), and O_2 represents the dissolved oxygen.

Oxygen inhibits denitrification while increasing NO_3^- , and temperature increases rate of denitrification. The effects of DO, temperature, and NO_3^- on denitrification were simulated using the inverse Michaelis-Menten equation (Chapelle, 1995):

$$N_D = -k_{N_2} \nu_D^{T-20} \left(\frac{K_{DO}}{K_{DO} + O_2} \right) NO_3 \quad (10)$$

where N_D represents the denitrification rate at the water-sediment interface ($mg \cdot L^{-1} \cdot d^{-1}$), NO_3 and O_2 are the near-bottom concentrations ($mg \cdot L^{-1}$), k_{N_2} is a coefficient that parameterises the effects of a characteristic local denitrification rate and an average rate of diffusion between the sediments and water (d^{-1}), ν_D is the temperature-rate coefficient for denitrification, T is water temperature ($^{\circ}C$), K_{DO} is the critical oxygen concentration for inhibition of denitrification ($mg \cdot L^{-1}$), O_2 represents the DO, and NO_3 represents NO_3^- -N content in field.

Table 1

Physicochemical properties of water and sediment in the field.

	Indicators	Month		
		June ^a	August ^a	December ^a
Water	T ^b ($^{\circ}C$)	27.23 ± 1.30	28.76 ± 1.38	3.93 ± 3.40
	EC ^b ($\mu s/cm$)	883.59 ± 327.51	598.90 ± 156.65	2181.34 ± 1157.65
	ORP ^b (mv)	342.81 ± 32.61	859.88 ± 124.49	-93.17 ± 29.06
	TDS ^b (g/L)	0.553 ± 0.21	0.36 ± 0.09	2.34 ± 0.99
	DO ^b (mg/L)	7.41 ± 2.73	6.47 ± 3.15	13.01 ± 1.81
	pH	9.19 ± 0.57	8.34 ± 0.50	6.91 ± 0.02
Sediment	PS ^b (μm)	19.19 ± 6.40	19.19 ± 6.47	19.50 ± 5.14
	pH	7.9 ± 0.50	8.15 ± 0.50	8.55 ± 0.45
	EC ($\mu s/cm$)	628.63 ± 335.00	280.02 ± 118.19	1228.33 ± 602.42

^a June represents the pre-concentrated rainfall period (low flow volume period), August represents the concentrated rainfall period (medium flow volume period), and December represents the water diversion period (high flow volume period).

^b T: Temperature; EC: Electrical conductivity; ORP: Redox potential; TDS: Total dissolved solids; DO: Dissolved oxygen; PS: Particle size.

2.3.4. Validation

To verify the accuracy of the N transport model proposed in this study, the total variation of NH_4^+ -N and NO_3^- -N in sediment was verified based on actual sampling data over a 30-day period. The validation results showed that the model fit accurately and predicted the N transport processes in the sediment for June, August, and December. The validation process is described in the Supplementary Material.

2.4. Microbial determination

2.4.1. DNA extraction and polymerase chain reaction (PCR) amplification

Total DNA was extracted from the sediment filtered through a 0.22 μm microfiltration membrane using a FastDNA® Spin Kit for Soil (MP Biomedicals, CA, U.S.), according to the manufacturer's instructions. The DNA extract was analysed on a 1 % agarose gel, and DNA concentration and purity were determined using a NanoDrop 2000 UV-VIS spectrophotometer (Thermo Scientific, Wilmington, DE, USA).

The V3-V4 hypervariable regions of the bacterial 16S rRNA gene were amplified with primers 338F (5'-ACTCCTACGGGAGGCGAGCAG-3')/806R (5'-GGACTACHVGGGTWTCTAAT-3') (Xu et al., 2016) using an ABI GeneAmp® 9700 PCR thermocycler (ABI, CA, USA). The PCR conditions were: 3 min of denaturation of template DNA at 95 °C, 27 cycles of 30 s at 95 °C, 30 s for annealing at 55 °C, and 45 s for elongation at 72 °C, and a final extension at 72 °C for 10 min.

2.4.2. Illumina MiSeq sequencing

Amplicons from each PCR sample were normalised to equimolar amounts and sequenced using 468-bp chemistry on a MiSeq PE300 platform (Illumina, San Diego, CA, USA) at Majorbio Bio-Pharm Technology Co. Ltd. (Shanghai, China). The sequencing data were submitted to the National Centre for Biotechnology Information's Sequence Read Archive database under accession number PRJNA811317. Subsequently, 16S rRNA sequencing data were processed using the MOTHUR MiSeq pipeline; details are provided in the Supplementary Information (Kozich et al., 2013).

2.5. Statistical analysis

To analyse the high-throughput data, quantitative insights into microbial ecology (QIIME) version 1.9.1 was used to classify the sequences into operational taxonomic units (OTUs) using a 97 % identity threshold (Caporaso et al., 2010). The α -diversity, Sobs, Shannon, and coverage indices were calculated using MOTHUR (Schloss et al., 2009). R language tools were then used to create rarefaction curves. Based on the data tables in the tax_summary_a folder, multi-level species and sunburst plots were drawn using R language tools to demonstrate the community composition of

microbial samples at the minimum genus level (Sui et al., 2016). Based on the 16S sequencing results, the PICRUST software package was used to predict the functional gene composition of the microbial community in water and sediment samples. Screening for functional genes associated with nitrification, denitrification and mineralisation processes at the KO level, followed by calculation of their cumulative abundance. The results were plotted using Origin version 2018 (OriginLab Inc., Northampton, MA, USA) as cumulative histograms (Sodhi et al., 2021).

3. Results

3.1. Nitrogen distribution in water and sediment

The flow volume of the Fu River varied with seasonal variations and the operational status of water diversion (Fig. 2). The average value of flow volume was the lowest ($2.10 \text{ m}^3/\text{s}$) in June, slightly higher ($2.34 \text{ m}^3/\text{s}$) in August, and the highest ($3.83 \text{ m}^3/\text{s}$) in December. Seasonal variations in the water temperature were also evident. The water temperature did not fluctuate significantly during the rainy season, remaining at approximately $28 \text{ }^\circ\text{C}$. It dropped to $3.93 \text{ }^\circ\text{C}$ during the water transfer period in winter (Table 1).

TN content in water ranged from 3.01 to 8.86 mg/L (mean 5.12 mg/L), 3.13 to 5.67 mg/L (mean 4.02 mg/L), and 1.55 to 12 mg/L (mean 7.29 mg/L) in June, August and December, respectively. The TN concentration in August decreased by 21.48% due to concentrated rainfall and increased by 42.38% in December due to water diversion, compared to that in June before the concentrated rainfall period. TN and $\text{NO}_3^- \text{-N}$ concentrations showed decreasing trend from F2 to F5, except for sites F1-1 and F1, where the water sources of the tributaries were different. The predominant forms of N in water were $\text{NO}_3^- \text{-N}$ and $\text{NO}_2^- \text{-N}$ in June, $\text{NH}_4^+ \text{-N}$ in August, and $\text{NO}_3^- \text{-N}$ and $\text{NH}_4^+ \text{-N}$ in December.

TN content in sediment during different sampling periods was also pronounced, ranging from 583.00 to 3263.10 mg/kg (mean 1581.44 mg/kg), 299.00 to 2320.00 mg/kg (mean 1319.00 mg/kg), and 815 to 2920 mg/kg (mean 1810.88 mg/kg) in June, August and December, respectively. The TN content of the sediment decreased by 16.60% in August and increased by 14.51% in December compared with that in June. The dominant form of N in the sediment was organic N, followed by $\text{NH}_4^+ \text{-N}$. The highest and lowest contents of $\text{NO}_3^- \text{-N}$ and $\text{NO}_2^- \text{-N}$ were observed in August and December, respectively.

These differences suggest that the transport and transformation processes of N at the water-sediment interface vary considerably under different hydrodynamic conditions.

3.2. Nitrogen transport processes

N fluxes of $\text{NH}_4^+ \text{-N}$ and $\text{NO}_3^- \text{-N}$ between water and sediment in the Fu River for different sampling periods are shown in Fig. 3, calculated from Eqs. (1) and (4), respectively. Controlled by concentration gradients, the fluxes of $\text{NH}_4^+ \text{-N}$ between the water and sediment interface were positive in all studied periods, indicating that $\text{NH}_4^+ \text{-N}$ was released from sediment to water (Fig. 3a). The mean $\text{NH}_4^+ \text{-N}$ release flux in June was $3.90 \text{ mg}\cdot\text{m}^{-2}\cdot\text{d}^{-1}$, which decreased to $3.75 \text{ mg}\cdot\text{m}^{-2}\cdot\text{d}^{-1}$ and $2.40 \text{ mg}\cdot\text{m}^{-2}\cdot\text{d}^{-1}$ in August and December, respectively. This suggests that an increase in flow reduces the release of $\text{NH}_4^+ \text{-N}$ caused by the concentration gradient. The flux of $\text{NO}_3^- \text{-N}$ was positive in June and December (mean flux of 1.25 and $0.15 \text{ mg}\cdot\text{m}^{-2}\cdot\text{d}^{-1}$, respectively, Fig. 3b), while it was negative in August (mean flux of $-0.74 \text{ mg}\cdot\text{m}^{-2}\cdot\text{d}^{-1}$), indicating that the sediment changed from a 'source' of $\text{NO}_3^- \text{-N}$ to a 'sink' of $\text{NO}_3^- \text{-N}$ due to the concentrated rainfall, and became a 'source' again during periods of water transfer. Under static release conditions, the release flux of $\text{NH}_4^+ \text{-N}$ was significantly greater than that of $\text{NO}_3^- \text{-N}$.

Controlled by resuspension processes, $\text{NH}_4^+ \text{-N}$ flux was positive and $\text{NO}_3^- \text{-N}$ flux was negative, indicating that the desorption capacity of $\text{NH}_4^+ \text{-N}$ for resuspended particles was greater than the adsorption capacity, whereas the opposite was true for $\text{NO}_3^- \text{-N}$ (Fig. 3). The release flux by resuspension was an order of magnitude greater than that by the concentration gradient (approximately $10\text{--}30$ times for $\text{NH}_4^+ \text{-N}$ and $25\text{--}2300$ times for $\text{NO}_3^- \text{-N}$), which indicates that the increased flow volume led to a considerable release of $\text{NH}_4^+ \text{-N}$ from sediment and settling of $\text{NO}_3^- \text{-N}$ to sediment by enhancing the resuspension process. This phenomenon is similar to the results obtained by Rysgaard and Berg (1996) and Wang et al. (2017). For $\text{NH}_4^+ \text{-N}$, the mean fluxes were $19.67 \text{ mg}\cdot\text{m}^{-2}\cdot\text{d}^{-1}$, $29.11 \text{ mg}\cdot\text{m}^{-2}\cdot\text{d}^{-1}$, and $233.71 \text{ mg}\cdot\text{m}^{-2}\cdot\text{d}^{-1}$ in June, August, and December, respectively. For $\text{NO}_3^- \text{-N}$, the average values of fluxes were $-25.30 \text{ mg}\cdot\text{m}^{-2}\cdot\text{d}^{-1}$, $-21.04 \text{ mg}\cdot\text{m}^{-2}\cdot\text{d}^{-1}$, and $-345.56 \text{ mg}\cdot\text{m}^{-2}\cdot\text{d}^{-1}$ in June, August, and December, respectively.

The total fluxes of $\text{NH}_4^+ \text{-N}$ between water and sediment by the concentration gradient and resuspension process were positive, while those of $\text{NO}_3^- \text{-N}$ were negative, suggesting that the Fu River sediment was a source of $\text{NH}_4^+ \text{-N}$ and a sink for $\text{NO}_3^- \text{-N}$ (Fig. 3). Concentrated rainfall affected the fluxes of $\text{NH}_4^+ \text{-N}$ and $\text{NO}_3^- \text{-N}$ slightly, whereas anthropogenic water diversion had a dramatic effect. The mean fluxes of $\text{NH}_4^+ \text{-N}$ were $24.13 \text{ mg}\cdot\text{m}^{-2}\cdot\text{d}^{-1}$, $32.86 \text{ mg}\cdot\text{m}^{-2}\cdot\text{d}^{-1}$, and $236.11 \text{ mg}\cdot\text{m}^{-2}\cdot\text{d}^{-1}$ in June, August, and December, respectively, whereas the mean fluxes of $\text{NO}_3^- \text{-N}$ were $-23.75 \text{ mg}\cdot\text{m}^{-2}\cdot\text{d}^{-1}$, $-21.78 \text{ mg}\cdot\text{m}^{-2}\cdot\text{d}^{-1}$, and $-345.41 \text{ mg}\cdot\text{m}^{-2}\cdot\text{d}^{-1}$ in June, August, and December, respectively. The fluxes of $\text{NO}_3^- \text{-N}$ responded more significantly to high flow volumes. This suggests

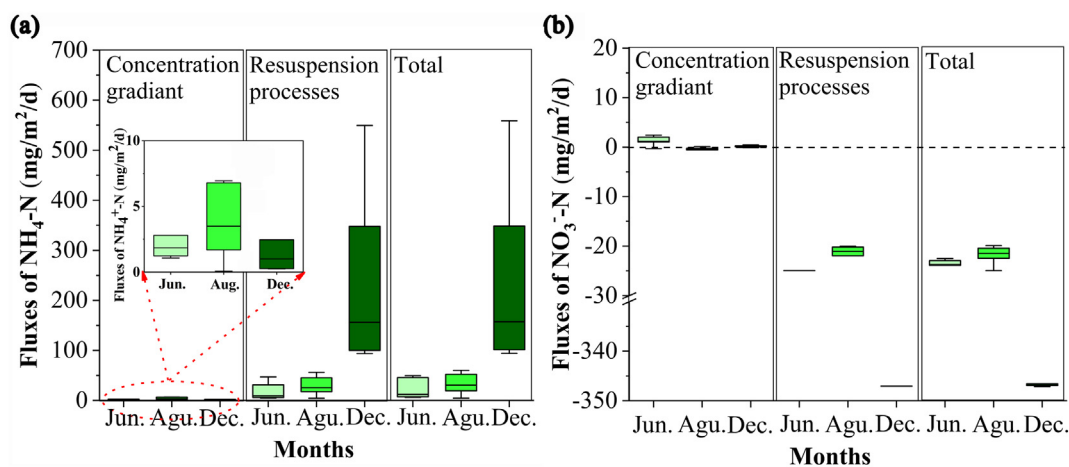


Fig. 3. Nitrogen fluxes of $\text{NH}_4^+ \text{-N}$ (a) and $\text{NO}_3^- \text{-N}$ (b) between water and sediment caused by concentration gradients and resuspension, separately and together before (June) and during concentrated rainfall (August), and water diversion period (December). Positive values of release flux represent the release of nitrogen from sediment to water while negative values represent the sedimentation of nitrogen from water to sediment.

that dramatic increase in river flow volume accelerates N transport processes at the water-sediment interface, posing a significant threat to water quality. However, the average flux of $\text{NO}_3^- \text{-N}$ decreased slightly during periods of concentrated rainfall, suggesting that the factors influencing changes in $\text{NO}_3^- \text{-N}$ fluxes when the flow volume increased slightly were complex and need to be studied in conjunction with N transformation processes at the water-sediment interface.

3.3. Nitrogen transformation processes

Fig. 4 represents the results of the nitrification, denitrification, and mineralisation rates in the Fu River sediments calculated using Eqs. (7), (9), and (10). At the river water-sediment interface, mineralisation was the dominant N transformation process, followed by denitrification (Fig. 4a, b, and c). The nitrification rate was the lowest. In Fu River, the average mineralisation, denitrification, and nitrification rates ranged from $342.68\text{--}29,170.49 \text{ mg}\cdot\text{L}^{-1}\cdot\text{d}^{-1}$, $11.57\text{--}467.42 \text{ mg}\cdot\text{L}^{-1}\cdot\text{d}^{-1}$, to $0.006\text{--}7.117 \text{ mg}\cdot\text{L}^{-1}\cdot\text{d}^{-1}$, respectively.

During periods of concentrated rainfall and water diversion, nitrification, denitrification, and mineralisation processes showed significant temporal variations. Due to concentrated rainfall, nitrification rates in sediment increased by approximately 42 times from June (mean $0.016 \text{ mg}\cdot\text{L}^{-1}\cdot\text{d}^{-1}$) to August (mean $0.682 \text{ mg}\cdot\text{L}^{-1}\cdot\text{d}^{-1}$), while denitrification rates remained almost unchanged (mean $30.42 \text{ mg}\cdot\text{L}^{-1}\cdot\text{d}^{-1}$ in June and $32.91 \text{ mg}\cdot\text{L}^{-1}\cdot\text{d}^{-1}$ in August). During the water diversion period, nitrification and denitrification rates in sediment increased by approximately 2980 times (mean $3.88 \text{ mg}\cdot\text{L}^{-1}\cdot\text{d}^{-1}$) and 523 times (mean $327.55 \text{ mg}\cdot\text{L}^{-1}\cdot\text{d}^{-1}$), respectively. Mineralisation rates in sediment decreased by 61.57 % during concentrated rainfall period (mean $13,581.84 \text{ mg}\cdot\text{L}^{-1}\cdot\text{d}^{-1}$ in June and mean $5218.60 \text{ mg}\cdot\text{L}^{-1}\cdot\text{d}^{-1}$ in August) and by 94.28 % during the period of water diversion (mean $776.66 \text{ mg}\cdot\text{L}^{-1}\cdot\text{d}^{-1}$ in December). Rising flow volume increased the rates of nitrification and denitrification in the sediment; however, it decreased the rate of mineralisation.

In contrast, the average $\text{NH}_4^+ \text{-N}$ and $\text{NO}_3^- \text{-N}$ transport rates at the river water-sediment interface were $21.74 \text{ mg}\cdot\text{L}^{-1}\cdot\text{d}^{-1}$ and $24.72 \text{ mg}\cdot\text{L}^{-1}\cdot\text{d}^{-1}$ in June, $32.86 \text{ mg}\cdot\text{L}^{-1}\cdot\text{d}^{-1}$ and $21.78 \text{ mg}\cdot\text{L}^{-1}\cdot\text{d}^{-1}$ in August, and $236.11 \text{ mg}\cdot\text{L}^{-1}\cdot\text{d}^{-1}$ and $345.41 \text{ mg}\cdot\text{L}^{-1}\cdot\text{d}^{-1}$ in December, respectively. These numbers far exceed the nitrification rates and are almost equal to denitrification rates. Therefore, the effects of physical transport and biochemical reactions of $\text{NH}_4^+ \text{-N}$ and $\text{NO}_3^- \text{-N}$ on N fluxes at the Fu River water-sediment interface cannot be ignored.

3.4. Overview of microbial community in water and sediment

To further investigate the mechanisms of biochemical reactions affecting N fluxes at the Fu River water-sediment interface, 75,758,512 high-quality 16S rRNA sequences were generated from 174 samples. After subsampling each sample to an equal sequencing depth (over 30,000

reads per sample) and clustering, 23,336 OTUs were obtained with 97 % identity, and the number of OTUs ranged from 1869 to 3020 per sample for sediment microorganisms and from 183 to 1868 per sample for water microorganisms (Supplementary Table 1). Good's coverage for the observed OTUs was approximately 92 % and 97 % in water and sediment, respectively, with rarefaction curves showing a clear asymptote (Supplementary Fig. 3), which together indicated near complete sampling of the community. In addition, the microbial number of OTUs, diversity, and community composition in the water and sediment were similar in June and August, while dramatic changes occurred in December (Supplementary Fig. 4).

3.5. Microbial nitrogen functional gene prediction

The relative abundance of functional microbial genes in water and sediment was predicted at the KO level to explain the rates of mineralisation, nitrification, and denitrification processes at the water-sediment interface. Overall, the relative abundance of microbial mineralisation, nitrification, and denitrification functional genes showed a pattern of low in June, high in August, and low again in December (Fig. 5). In addition, the relative abundances of mineralisation- and denitrification-related functional genes were almost identical in the water and sediment. In June and August, the functional genes associated with nitrification dominated the sediment; and in December, their relative abundance decreased in the sediment and increased in the water.

The sediment microbial community had the highest relative abundance of mineralisation functional genes, followed by denitrification functional genes and nitrification functional genes. The relative abundances of functional genes related to mineralisation ranged from approximately 0.021 to 0.024 for sediment microbes, 0.000009 to 0.00003 for nitrification, and 0.0116 to 0.0119 for denitrification.

4. Discussion

4.1. Slight or dramatic flow volume increases had different effects on N transport processes at the river water-sediment interface

It is generally accepted that increased flow volume leads to increased N release from the sediment due to the increased static release of N controlled by concentration gradients and increased N transport controlled by resuspension processes (Tong et al., 2016). The input of large volumes of fresh water over a short period of time, such as concentrated rainfall and artificial water transfers, strongly dilutes river water, resulting in a decrease in the TN content of the water. The increased N concentration gradient between water and sediment promotes the static release of N (Arheimer et al., 1996; Caffrey and Day, 1986). At the same time, elevated flow volume effectively increases resuspension fluxes and N release from sediments (Depinto et al., 1994; Kelderman et al., 2012; Wang et al., 2013). Therefore,

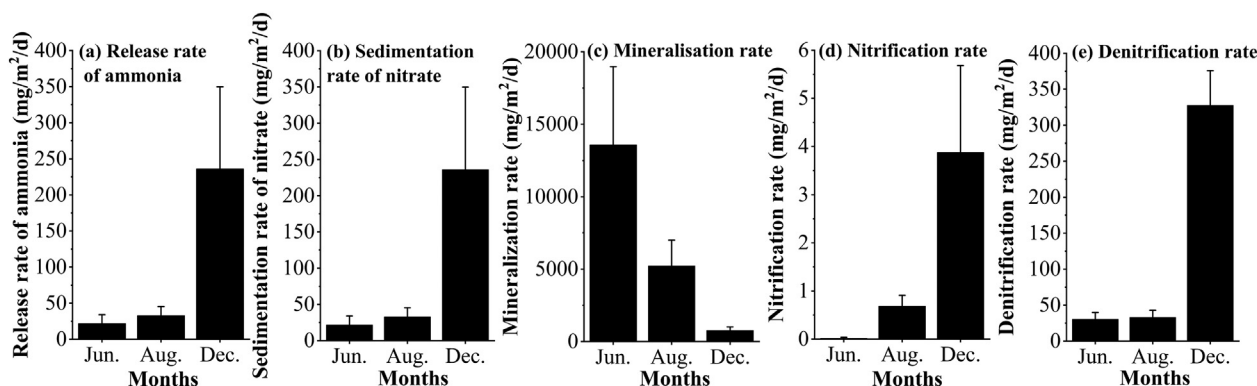


Fig. 4. Rates of release of $\text{NH}_4^+ \text{-N}$ (a) in sediments, sedimentation of $\text{NO}_3^- \text{-N}$ (b), nitrification (c), denitrification (d), mineralisation (e) in sediments at each monitoring section along the Fu River before (June) and during concentrated rainfall (August), and water diversion period (December).

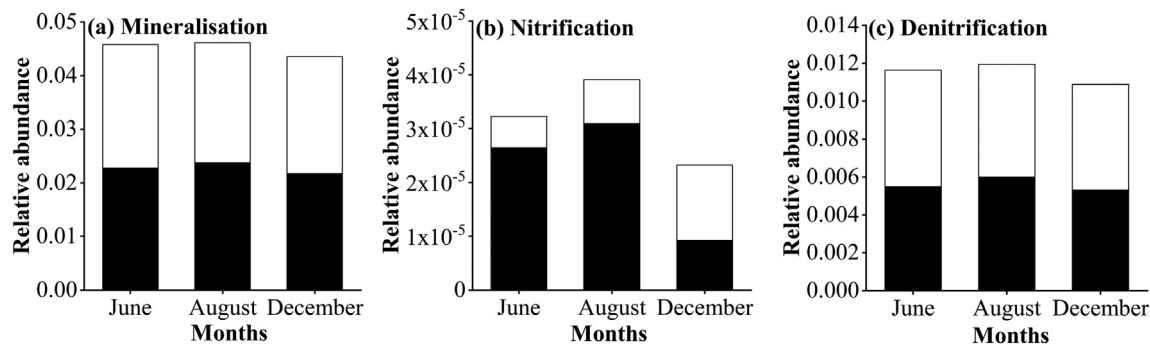


Fig. 5. Predicted relative abundance of microbial mineralisation (a), nitrification (b), and denitrification (c) functional genes in Fu River sediments before (June) and during concentrated rainfall (August), and water diversion period (December).

in previous studies, inorganic N release fluxes at the water-sediment interface have been positively correlated with flow volume.

However, in this study, NH_4^+ -N and NO_3^- -N responded differently to increased flow volumes. Compared with June, the flow volume increased by 11.43 % and 82.38 % in August and December, respectively. As the flow volume increased, NH_4^+ -N tended to transfer from the sediment to the water, whereas NO_3^- -N followed the other way round. This tendency was also reported in the Yellow River (Cheng et al., 2015a) and Yangtze River (Cheng et al., 2015b). Scientists have speculated that this phenomenon is caused by a combination of the sediment N content and pH value. Slightly alkaline sediments can facilitate the release of NH_4^+ -N from the sediment to water (Yu et al., 2015). In nitrogen-rich rivers, NO_3^- -N tends to settle from the water into the sediment (Lefebvre et al., 2004). The Fu River sediment has a pH value >8 (Table 1) with a long history of N accumulation, making it a nitrogen-rich river (Jun et al., 2010).

At the same time, slight and dramatic increases in flow had different effects on NH_4^+ -N and NO_3^- -N fluxes at the water-sediment interface. A slight increase in the flow volume caused by concentrated rainfall accelerated the release of NH_4^+ -N (by 36.15 %); however, it inhibited the sedimentation of NO_3^- -N (by 17.56 %). The dramatic increase in flow volume due to water transfer caused a significant increase in NH_4^+ -N release (by 878.31 %) and NO_3^- -N sedimentation (by 1555.18 %). The reasons for this include streambed particle redistribution and dilution processes, and properties of NH_4^+ -N and NO_3^- -N.

The slight increase in flow volume facilitated the redistribution of river sediment particles, resulting in a smaller mean PS and reduced porosity of sediment particles in the lower section of the Fu River, thereby inhibiting molecular diffusion of the pore water, which is controlled by concentration gradients of NH_4^+ -N and NO_3^- -N. The data from this study showed that the porosity of the water-sediment interface was reduced by nearly 100 %. The concentration gradient-controlled release efficiency of NH_4^+ -N and NO_3^- -N decreased from $3.90 \text{ mg}\cdot\text{m}^{-2}\cdot\text{d}^{-1}$ to $3.75 \text{ mg}\cdot\text{m}^{-2}\cdot\text{d}^{-1}$ and from $1.25 \text{ mg}\cdot\text{m}^{-2}\cdot\text{d}^{-1}$ (sediment as 'source') to $-0.74 \text{ mg}\cdot\text{m}^{-2}\cdot\text{d}^{-1}$ (sediment as 'sink'), respectively, after concentrated rainfall. Water diversion resulted in a sharp increase in the flow volume, which strongly diluted the river water. Compared to June, the NO_3^- -N concentration in the water decreased by approximately 70.78 % owing to dilution. Therefore, it was presumed that the sediment NO_3^- -N pore-water release process was enhanced. In addition, the rate of NH_4^+ -N release from pore water might have been inhibited by low temperatures ($3.93 \text{ }^\circ\text{C}$ in December) by $2.40 \text{ mg}\cdot\text{m}^{-2}\cdot\text{d}^{-1}$.

In natural rivers with evident hydrodynamic disturbances, resuspension is the main mechanism causing changes in water-sediment N fluxes compared to concentration gradients (Qian et al., 2011). In general, an increase in the flow volume can lead to a rapid increase in the inorganic N release. However, once a critical flow is reached, the inorganic N resolution/absorption process becomes important, resulting in fluxes that remain constant or decrease slightly (Zhong et al., 2017; Yu et al., 2017). The data from this study showed that both slight and dramatic flow volume increases, caused by concentrated rainfall and water transfer, respectively, promoted the desorption of NH_4^+ -N at the water-sediment interface

(47.95 % and 1087.94 % increase, respectively); however, they inhibited and promoted the sedimentation process of NO_3^- -N (16.85 % decrease and 1265.63 % increase, respectively). This might indicate that the critical flow volume of NH_4^+ -N was high and it was released at the water-sediment interface with a slight or dramatic flow volume increase. In turn, a slight increase in flow volume due to concentrated rainfall reached the critical flow volume for the NO_3^- -N sedimentation process, causing a decrease in NO_3^- -N sedimentation. However, when the flow volume increased dramatically due to water transfer, the rate of NO_3^- -N sedimentation increased further, indicating the possibility of a staged equilibrium flux of NO_3^- -N exchange in the flowing water system, that is, the flow volume continued to increase dramatically after the reaching a critical value, and eventually the flux of N exchange increased.

Overall, a slight increase in the flow volume resulted in an increase in the flux of NH_4^+ -N release and a decrease in the flux of NO_3^- -N sedimentation at the water-sediment interface. Dramatic increases in flow volume resulted in a simultaneous increase in NH_4^+ -N release and NO_3^- -N sedimentation at the water-sediment interface. This phenomenon is mediated by several processes, including the redistribution of sediment particles, dilution, and adsorption and desorption of N. This suggests that slight and dramatic increases in flow volume could affect the fluxes of NH_4^+ -N and NO_3^- -N caused by pore water release and resuspension at the water-sediment interface by different mechanisms.

4.2. Slight or dramatic flow volume increases had different effects on nitrogen transformation processes at the water-sediment interface

N transformation processes in aquatic environments are mediated by key microorganisms. Of these, mineralisation, nitrification, and denitrification have received much attention because of their ability to significantly influence the amount of N and transformation of N forms in water. The efficiency of mineralisation, nitrification, and denitrification is reported to be proportional to the relative levels of functional genes associated with microorganisms. Therefore, the composition of functional genes is an indicator of N transformation processes in aqueous environments. In the present study, the relative abundance of nitrogen-related functional genes was low in June, high in August, and low in December, which is justified by the promotion of microbial colonisation via external loading of N due to high temperatures, increased flow volume, and soil flushing during periods of concentrated rainfall, whereas the lower temperature in December ($3.93 \text{ }^\circ\text{C}$) inhibited the activity of most microorganisms. However, model simulations of the efficiency of mineralisation, nitrification, and denitrification processes showed that the efficiency of mineralisation decreased by 94.28 % with increasing flow volume, whereas the efficiency of nitrification and denitrification increased significantly (2980 and 523 times, respectively). This indicates that the efficiency of N transformation in an aqueous environment is controlled by both the relative abundance of nitrogen-related functional genes and flow volume.

Long hydraulic residence times are one of the main factors affecting mineralisation rates in sediments (Sundbäck et al., 1990). The hydraulic

residence time decreased considerably with increasing flow volume, leading to a continuous decrease in mineralisation rates at the water-sediment interface during periods of concentrated rainfall and water delivery (Fig. 3c). The efficiency of the nitrification and denitrification processes was closely related to the flow volume, which significantly influenced the N release from the water-sediment interface. Nitrification occurred in the aerobic surface zone, whereas denitrification occurred in the anoxic zone, with a maximum thickness of a few millimetres for both the zones (Zheng et al., 2019). Abril et al. (2000) suggested that in rivers, nitrification processes occur in oxygenated water, whereas denitrification occurs in oxygenated mud. At the same time, high flow rates would promote microbial activity at the river water-sediment interface because microorganisms prefer to settle on resuspended particles (Fries et al., 2008). Thus, at high flow volume, the resuspension process intensified, the nitrification and denitrification zones, i.e. the mixed layer of water and mud, became thicker. Microorganisms move frequently with the resuspended particles and the probability of contacting the reaction feedstock (NH_4^+ -N and NO_3^- -N) rose, potentially leading to a much higher rate of nitrification and denitrification in the sediment. This study found that both slight and dramatic flow volume increases significantly inhibit the mineralisation process because the microorganisms do not have sufficient time to come into contact with organic particulate matter. Slight flow increases did not contribute significantly to the efficiency of nitrification and denitrification processes, whereas a dramatic increase in flow volume did. Therefore, when using nitrogen-related functional genes of river microbial communities to infer spatial and temporal changes in the efficiency of N cycling processes, attention should also be paid to changes in river flow volume.

4.3. Impacts on aquatic environmental restoration and management

River sediments are always weakly alkaline and are, therefore, always a source of NH_4^+ -N (Fanning and Pilon, 1971). In nitrogen-rich rivers, sediments tend to act as NO_3^- -N sinks. This study showed that a slight increase in flow volume promoted the release of NH_4^+ -N from the sediment, inhibited NO_3^- -N sedimentation, reduced mineralisation rates, promoted nitrification processes, and had little effect on denitrification rates. Ultimately, a high-N load was imposed on the river water. The dramatic increase in flow volume resulted in a simultaneous increase in NH_4^+ -N release and NO_3^- -N sedimentation at the water-sediment interface, an evident decrease in mineralisation rates, and a noticeable increase in both nitrification and denitrification rates. Therefore, a dramatic increase in flow volume inhibited inorganic N production and promoted inorganic N consumption, resulting in a transient low inorganic N load in the aquatic environment. This hints at a potential global N sink that may have been overlooked in the past. However, by drastically increasing the concentration of resuspended particles, the water transfer project significantly increased the TN loading in the short term, leading to the deterioration of water quality in the water receiving area. Thus, flow volume control is important when planning water-transfer projects.

NH_4^+ -N and NO_3^- -N, as the main inorganic forms of N, are important contributors to excess N in water. To the best of our knowledge, this is the first study to use a combination of modelling and microbial sequencing techniques to systematically analyse the impact of slight and dramatic flow volume increases on water-sediment N transport and transformation. This study suggests that in large-scale anthropogenic regulation of rivers, such as reservoir management and diversion planning, consideration should be given to the rational allocation of flow volume across the seasons to reduce the overall N load to nitrogen-rich rivers. A solution was provided to address the phenomenon of re-pollution of water during the implementation of reservoir management and water transfer projects. New ideas were provided to prevent eutrophication.

5. Conclusions

To address the failure of water environment management policies, a model of N transport and transformation at the river water-sediment

interface was constructed based on hydrodynamic models and biochemical reaction models. This model was proposed to assess the response of N loading to river waters to slight or and dramatic increases in river flow volume caused by natural factors (concentrated rainfall) and anthropogenic factors (large hydraulic projects) contributed by sediment. It emphasises the importance of flow volume control in river environmental management.

The results of this study showed that a slight increase in flow volume promoted the release of NH_4^+ -N from sediment but prevented the sedimentation of NO_3^- -N in water, increasing the inorganic N load to the river water. A dramatic increase in flow volume simultaneously promoted nitrification-denitrification processes, leading to inorganic N consumption increasing. In large-scale anthropogenic regulation of rivers, such as reservoir management and water transfers, rational flow volume allocation across seasons should be considered to reduce the overall N load to nitrogen-rich river. This study provides a solution to the phenomenon of river re-pollution in nitrogen-rich rivers. At the same time, these results also suggest that the enhanced denitrification due to dramatic increase in flow volume is a potential global nitrogen sink that may have been overlooked.

Furthermore, possible changes in the relative abundance of functional microbial genes based on high-throughput sequencing techniques suggested the efficiency of N transformation processes in aquatic environments was controlled by the relative abundance of nitrogen-related functional genes and flow volume, and changes in river flow volume should be taken into account when using nitrogen-related functional genes of microbial communities to infer spatial and temporal changes in the efficiency of N cycling.

CRediT authorship contribution statement

Jiali Lü: Conceptualization, Data curation, Methodology, Formal analysis, Writing - original draft preparation, Writing - review and editing, Supervision. **Shiqin Wang:** Conceptualization, Data curation, Writing - Original draft preparation. Methodology, Formal analysis, Supervision. Funding acquisition. **Binbin Liu:** Conceptualization, Supervision. **Wenbo Zheng:** Investigation **Kangda Tan:** Investigation. **Xianfang Song:** Methodology.

Funding

This work was supported by the National Key Research and Development Program of China (2021YFD1700500), the National Natural Science Foundation of China (No. 42071053) and the National Science Foundation for Distinguished Young Scholars of Hebei Province of China (No. D2019503072).

Declaration of competing interest

The authors declare that they have no known competing financial interests or personal relationships that could have appeared to influence the work reported in this paper.

Acknowledgements

The views and rationale presented in this manuscript are those of the authors and do not necessarily represent the funding agency.

Appendix A. Supplementary data

Supplementary data to this article can be found online at <https://doi.org/10.1016/j.scitotenv.2022.157013>.

References

- Abril, G., Riou, S.A., Etcheber, H., Frankignoulle, M., de Wit, R., Middelburg, J.J., 2000. Transient, tidal time-scale, nitrogen transformations in an estuarine turbidity maximum—fluid mud system (The Gironde, South-west France). *Estuar. Coast. Shelf S.* 50 (5), 703–715.

- Alexander, R.B., Böhlke, J.K., Boyer, E.W., David, M.B., Harvey, J.W., Mulholland, P.J., Seitzinger, S.P., Tobias, C.R., Tonitto, C., Wollheim, W.M., 2009. Dynamic modeling of nitrogen losses in river networks unravels the coupled effects of hydrological and biogeochemical processes. *Biogeochemistry* 93 (1), 91–116.
- Arheimer, B., Andersson, L., Lepistö, A., 1996. Variation of nitrogen concentration in forest streams — influences of flow, seasonality and catchment characteristics. *J. Hydrol.* 179 (1), 281–304.
- Ballantine, D.J., Davies-Colley, R.J., 2013. Nitrogen, phosphorus and E. coli loads in the Sherry River, New Zealand. *N.Z.J. Mar. Freshw.* 47 (4), 529–547.
- Brase, L., Sanders, T., Dähnke, K., 2018. Anthropogenic changes of nitrogen loads in a small river: external nutrient sources vs. internal turnover processes. *Isot. Environ. Health. Stud.* 54 (2), 168–184.
- Brigolin, D., Lovato, T., Rubino, A., Pastres, R., 2011. Coupling early-diagenesis and pelagic biogeochemical models for estimating the seasonal variability of N and P fluxes at the sediment–water interface: Application to the northwestern Adriatic coastal zone. *J. Marine Syst.* 87 (3–4), 239–255.
- Bustillo, V., Victoria, R., Moura, J.M., Victoria, D., Toledo, A., Colicchio, E., 2011. Biogeochemistry of carbon in the amazonian floodplains over a 2000-km reach: insights from a process-based model. *Earth Interact.* 15.
- Caffrey, J.M., Day, J.W., 1986. Control of the variability of nutrients and suspended sediments in a gulf coast estuary by climatic forcing and spring discharge of the Atchafalaya River. *Estuaries* 9 (4), 295.
- Campos, M., Rilling, J.I., Acuña, J.J., Valenzuela, T., Larama, G., Peña-Cortés, F., Ogram, A., Jaisi, D.P., Jorquera, M.A., 2021. Spatiotemporal variations and relationships of phosphorus, phosphomonoesterases, and bacterial communities in sediments from two Chilean rivers. *Sci. Total Environ.* 776, 145782.
- Caporaso, J.G., Kuczynski, J., Stombaugh, J., Bittinger, K., Bushman, F.D., Costello, E.K., Fierer, N., Peña, A.G., Goodrich, J.K., Gordon, J.L., Huttley, G.A., Kelley, S.T., Knights, D., Koenig, J.E., Ley, R.E., Lozupone, C.A., McDonald, D., Muegge, B.D., Pirrung, M., Reeder, J., Sevinsky, J.R., Turnbaugh, P.J., Walters, W.A., Widmann, J., Yatsunami, T., Zaneveld, J., Knight, R., 2010. QIIME allows analysis of high-throughput community sequencing data. *Nat. Methods* 7 (5), 335–336.
- Chapelle, A., 1995. A preliminary model of nutrient cycling in sediments of a Mediterranean lagoon. *Ecol. Model.* 80 (2), 131–147.
- Chen, D., Huang, H., Hu, M., Dahlgren, R.A., 2014. Influence of lag effect, soil release, and climate change on watershed anthropogenic nitrogen inputs and riverine export dynamics. *Environ. Sci. Technol.* 48 (10), 5683–5690.
- Cheng, X., Hou, L., Liu, M., Zheng, Y., Yin, G., Li, X., Gao, J., Deng, F., Jiang, X., 2015a. Inorganic nitrogen exchange across the sediment–water interface in the eastern Chongming tidal flat of the Yangtze Estuary. *Environ. Earth Sci.* 74 (3), 2173–2184.
- Cheng, X., Hou, L., Liu, M., Zheng, Y., Yin, G., Li, X., Gao, J., Deng, F., Jiang, X., 2015b. Inorganic nitrogen exchange across the sediment–water interface in the eastern Chongming tidal flat of the Yangtze Estuary. *Environ. Earth Sci.* 74 (3), 2173–2184.
- Conley, D.J., Paerl, H.W., Howarth, R.W., Boesch, D.F., Seitzinger, S.P., Havens, K.E., Lancelot, C., Likens, G.E., 2009. Controlling eutrophication: nitrogen and phosphorus. *Science* 323 (5917), 1014–1015.
- Czerwionka, K., 2016. Influence of dissolved organic nitrogen on surface waters. *Oceanologia* 58 (1), 39–45.
- Dagg, M.J., Ammerman, J.W., Amon, R.M.W., Gardner, W.S., Green, R.E., Lohrenz, S.E., 2007. A review of water column processes influencing hypoxia in the northern Gulf of Mexico. *Estuar. Coast.* 30 (5), 735–752.
- David, F., Marchand, C., Thiney, N., Nhu-Trang, T., Meziane, T., 2019. Short-term changes in the quality of suspended particulate matter in a human impacted and mangrove dominated tropical estuary (Can Gio, Vietnam). *Cont. Shelf Res.* 178, 59–67.
- Depinto, J., Lick, W., Paul, J., 1994. Transport and transformation of contaminants near the sediment–water interface. *Int. J. Proj.* 5 (25), 517–526.
- Fanning, K.A., Pilson, M.E., 1971. Interstitial silica and pH in marine sediments: some effects of sampling procedures. *Science* 173 (4003), 1228–1231.
- Ferguson, A.J.P., Oakes, J., Eyre, B.D., 2020. Bottom trawling reduces benthic denitrification and has the potential to influence the global nitrogen cycle. *Limnol. Oceanogr.* 5 (3), 237–245.
- Fries, J.S., Characklis, G.W., Noble, R.T., 2008. Sediment–water exchange of *Vibrio* sp. and fecal indicator bacteria: implications for persistence and transport in the Neuse River Estuary, North Carolina, USA. *Water Res.* 42 (4), 941–950.
- Gao, Y., Yu, J., Song, Y., Zhu, G., Paerl, H.W., Qin, B., 2019. Spatial and temporal distribution characteristics of different forms of inorganic nitrogen in three types of rivers around Lake Taihu, China. *Environ. Sci. Pollut. Res.* 26 (7), 6898–6910.
- Gao, Y., Zhang, W., Li, Y., Wu, H., Yang, N., Hui, C., 2021. Dams shift microbial community assembly and imprint nitrogen transformation along the Yangtze River. *Water Res.* 189, 116579.
- García, M., Parker, G., 1993. Experiments on the entrainment of sediment into suspension by a dense bottom current. *J. Geophys. Res.* 98, 4793–4808.
- Gayathri, S., Krishnan, K.A., Krishnakumar, A., Maya, T.M.V., Dev, V.V., Antony, S., Arun, V., 2021. Monitoring of heavy metal contamination in Netravati river basin: overview of pollution indices and risk assessment. *Sust. Wart. Resour. Man.* 7 (2), 20.
- Ha, M., Zhang, Z., Wu, M., 2018. Biomass production in the Lower Mississippi River Basin: mitigating associated nutrient and sediment discharge to the Gulf of Mexico. *Sci. Total Environ.* 635, 1585–1599.
- Harrison, L.R., Legleiter, C.J., Wyzga, M.A., Dunne, T., 2011. Channel dynamics and habitat development in a meandering gravel bed river. *Water Resour. Res.* 47 (4).
- Hiroshi, T., 1991. Double-plunger pump system flow injection spectrophotometric determination of inorganic nitrogen in soil extracts (Part 2): flow injection analysis of nitrate nitrogen in soil extracts. *J. Soil Sci. Plant Nutr.* 62 (2), 135–140.
- Hitchcock, J.N., Mitrovic, S.M., 2013. Different resource limitation by carbon, nitrogen and phosphorus between base flow and high flow conditions for estuarine bacteria and phytoplankton. *Estuar. Coast. Shelf Sci.* 135, 106–115.
- Hodgkins, R., Tranter, M., Dowdeswell, J.A., 1998. The hydrochemistry of runoff from a 'cold-based' glacier in the High Arctic (Scott Turnerbreen, Svalbard). *Hydrol. Process.* 12 (1), 87–103.
- Huang, X., 2017. Study on Nitrogen Forms and Adsorption-Desorption Characteristics of Nitrate Nitrogen in Sediment Xiangjiang River From Hengyang Section. Nanhua University Master.
- Huang, X., He, S., Wang, S., 2017. Characteristics of adsorption of nitrate nitrogen for the sediment substances in Hengyang section of Xiang River. *Ecotoxicol. Environ. Saf.* 17 (05), 1922–1926.
- Jun, W., Gao, G., Yuansheng, P., Zhifeng, Y., 2010. Sources and transformations of nitrogen in the Fuhe River of the Baiyangdian Lake (in China). *Environ. Sci.* 31 (12), 2905–2910.
- Karthäuser, C., Ahmerkamp, S., Marchant, H.K., Bristow, L.A., Hauss, H., Iversen, M.H., Kiko, R., Maerz, J., Lavik, G., Kuypers, M.M.M., 2021. Small sinking particles control anammox rates in the Peruvian oxygen minimum zone. *Nat. Commun.* 12 (1), 3235.
- Kaveeshwar, R., Cherian, L., Gupta, V.K., 1991. Extraction–spectrophotometric determination of nitrite using 1-aminonaphthalene-2-sulphonate. *Analyst* 116 (6), 667–669.
- Kelderman, P., Ang Weya, R.O., De Rozari, P., Vijverberg, T., 2012. Sediment characteristics and wind-induced sediment dynamics in shallow Lake Markermeer, the Netherlands. *Aquat. Sci.* 74 (2), 301–313.
- Kozich, J.J., Westcott, S.L., Baxter, N.T., Highlander, S.K., Schloss, P.D., 2013. Development of a dual-index sequencing strategy and curation pipeline for analyzing amplicon sequence data on the MiSeq Illumina sequencing platform. *Appl. Environ. Microb.* 79 (17), 5112–5120.
- Kuypers, M.M.M., Marchant, H.K., Kartal, B., 2018. The microbial nitrogen-cycling network. *Nat. Rev. Microbiol.* 16 (5), 263–276.
- Lefebvre, S., Marmonier, P., Pinay, G., 2004. Stream regulation and nitrogen dynamics in sediment interstices: comparison of natural and straightened sectors of a third-order stream. *River Res. Appl.* 20 (5), 499–512.
- Leu, H., Ouyang, C., Su, J., 1996. Effects of flow velocity changes on nitrogen transport and conversion in an open channel flow. *Water Res.* 30 (9), 2065–2071.
- Lin, J., Chen, N., Yuan, X., Tian, Q., Hu, A., Zheng, Y., 2020. Impacts of human disturbance on the biogeochemical nitrogen cycle in a subtropical river system revealed by nitrifier and denitrifier genes. *Sci. Total Environ.* 746, 141139.
- Lunau, M., Voss, M., Erickson, M., Dziallas, C., Casciotti, K., Ducklow, H., 2013. Excess nitrate loads to coastal waters reduces nitrate removal efficiency: mechanism and implications for coastal eutrophication. *Environ. Microbiol.* 15 (5), 1492–1504.
- Lv, J., Yuan, R., Wang, S., 2021. Water diversion induces more changes in bacterial and archaeal communities of river sediments than seasonality. *J. Environ. Manag.* 293, 112876.
- Malone, T.C., Newton, A., 2020. The globalization of cultural eutrophication in the coastal ocean: causes and consequences. *Front. Mar. Sci.* 7, 670.
- Meng, X., Zhang, W., Shan, B., 2020. Distribution of nitrogen and phosphorus and estimation of nutrient fluxes in the water and sediments of liangzi LakeChina. *Environ. Sci. Pollut. Res.* 27 (7), 7096–7104.
- Mihiranga, H.K.M., Jiang, Y., Li, X., Wang, W., De Silva, K., Kumwimba, M.N., Bao, X., Nissanka, S.P., 2021. Nitrogen/phosphorus behavior traits and implications during storm events in a semi-arid mountainous watershed. *Sci. Total Environ.* 791, 148382.
- Müller, B., Wang, Y., Dittrich, M., Wehrl, B., 2003. Influence of organic carbon decomposition on calcite dissolution in surficial sediments of a freshwater lake. *Water Res.* 37 (18), 4524–4532.
- Qian, J., Zheng, S., Wang, P., Wang, C., 2011. Experimental study on sediment resuspension in Taihu Lake under different hydrodynamic disturbances. *J. Hydrodyn.* 23 (6), 826–833.
- Queste, B.Y., Fernand, L., Jickells, T.D., Heywood, K.J., Hind, A.J., 2016. Drivers of summer oxygen depletion in the central North Sea. *Biogeosciences* 13 (4), 1209–1222.
- Räike, A., Taskinen, A., Knuuttila, S., 2020. Nutrient export from Finnish rivers into the Baltic Sea has not decreased despite water protection measures. *Ambio* 49 (2), 460–474.
- Reisinger, A.J., Groffman, P.M., Rosi-Marshall, E.J., 2016. Nitrogen-cycling process rates across urban ecosystems. *FEMS Microbiol. Ecol.* 92 (12), w198.
- Ren, C., Zhang, Q., Wang, H., Wang, Y., 2021. Identification of sources and transformations of nitrate in the intense human activity region of North China using a multi-isotope and Bayesian model. *Int. J. Environ. Res. Public Health* 18, 8642.
- Rysgaard, S., Berg, P., 1996. Mineralization in a northeastern Greenland sediment: mathematical modelling, measured sediment pore water profiles and actual activities. *Aquat. Microb. Ecol.* 11 (3), 297–305.
- Ryu, H., Kang, T., Kim, K., Nam, T., Han, Y., Kim, J., Kim, M., Lim, H., Seo, K., Lee, K., Yoon, S., Hwang, S.H., Na, E.H., Lee, J.H., 2021. Tracking nitrate sources in agricultural-urban watershed using dual stable isotope and Bayesian mixing model approach: considering N transformation by Lagrangian sampling. *J. Environ. Manag.* 300, 113693.
- Schacht, U., Wallmann, K., Kutterolf, S., Schmidt, M., 2008. Volcanogenic sediment–seawater interactions and the geochemistry of pore waters. *Chem. Geol.* 249 (3–4), 321–338.
- Schloss, P.D., Westcott, S.L., Ryabin, T., Hall, J.R., Hartmann, M., Hollister, E.B., Lesniewski, R.A., Oakley, B.B., Parks, D.H., Robinson, C.J., Sahl, J.W., Stres, B., Thallinger, G.G., Van Horn, D.J., Weber, C.F., 2009. Introducing mothur: open-source, platform-independent, community-supported software for describing and comparing microbial communities. *Appl. Environ. Microb.* 75 (23), 7537–7541.
- Serpa, D., Falcão, M., Duarte, P., Da Fonseca, L.C., Vale, C., 2007. Evaluation of ammonium and phosphate release from intertidal and subtidal sediments of a shallow coastal lagoon (Ria Formosa – Portugal): a modelling approach. *Biogeochemistry* 82 (3), 291–304.
- Shayo, S., Limbu, S.M., 2018. Nutrient release from sediments and biological nitrogen fixation: advancing our understanding of eutrophication sources in Lake Victoria, Tanzania. *Lakes Reserv. Sci. Policy Manag. Sustain. Use* 23 (4), 312–323.
- Singh, K.P., Malik, A., Mohan, D., Sinha, S., 2004. Multivariate statistical techniques for the evaluation of spatial and temporal variations in water quality of Gomti River (India)—a case study. *Water Res.* 38 (18), 3980–3992.
- Sodhi, K.K., Kumar, M., Singh, D.K., 2021. Assessing the bacterial diversity and functional profiles of the River Yamuna using Illumina MiSeq sequencing. *Arch. Microbiol.* 203 (1), 367–375.

- Stafilov, T., Špirić, Z., Glad, M., Barandovski, L., Bačeva Andonovska, K., Šajin, R., Antonić, O., 2020. Study of nitrogen pollution in the Republic of North Macedonia by moss biomonitoring and Kjeldahl method. *J. Environ. Sci. Health A* 55 (6), 759–764.
- Sui, Q., Liu, C., Zhang, J., Dong, H., Zhu, Z., Wang, Y., 2016. Response of nitrite accumulation and microbial community to free ammonia and dissolved oxygen treatment of high ammonium wastewater. *Appl. Microbiol. Biot.* 100 (9), 4177–4187.
- Sundbäck, K., Jönsson, B., Nilsson, P., Lindström, I., 1990. Impact of accumulating drifting macroalgae on a shallow-water sediment system: an experimental study. *Mar. Ecol. Prog. Ser.* 58 (3), 261–274.
- Tao, K., Liu, Y., Ke, T., Zhang, Y., Xiao, L., Li, S., Wei, S., Chen, L., Hu, T., 2019. Patterns of bacterial and archaeal communities in sediments in response to dam construction and sewage discharge in Lhasa River. *Ecotoxicol. Environ. Saf.* 178, 195–201.
- Tao, Y., Zhang, L., Su, Z., Dai, T., Zhang, Y., Huang, B., Wen, D., 2021. Nitrogen-cycling gene pool shrunk by species interactions among denser bacterial and archaeal community stimulated by excess organic matter and total nitrogen in a eutrophic bay. *Mar. Environ. Res.* 169, 105397.
- Tong, Y., Liang, T., Wang, L., Tian, S., 2016. Characteristics of nitrogen release from Lake Dongting sediments under variable water level and velocity in the two-way annular flume (in China). *J. Lake Sci.* 29 (01), 59–67.
- van der Wulp, S.A., Damar, A., Ladwig, N., Hesse, K.J., 2016. Numerical simulations of river discharges, nutrient flux and nutrient dispersal in Jakarta Bay, Indonesia. *Mar. Pollut. Bull.* 110 (2), 675–685.
- Vandenbruwane, J., De Neve, S., Qualls, R.G., Sleutel, S., Hofman, G., 2007. Comparison of different isotherm models for dissolved organic carbon (DOC) and nitrogen (DON) sorption to mineral soil. *Geoderma* 139 (1), 144–153.
- Wang, Z., Song, X., Li, G., Zhang, J., Yu, G., Sun, X., 2013. Variations of nitrogen transport in the mainstream of the Yellow River, China. *Int. J. Environ. Pollut.* 52 (1–2), 82–103.
- Wang, J., Zhao, Q., Pang, Y., Hu, K., 2017. Research on nutrient pollution load in Lake Taihu, China. *Environ. Sci. Pollut. Res.* 24 (21), 17829–17838.
- Wang, W.W., Jiang, X., Zheng, B.H., Chen, J.Y., Zhao, L., Zhang, B., Wang, S.H., 2018. Composition, mineralization potential and release risk of nitrogen in the sediments of Keluke Lake, a Tibetan Plateau freshwater lake in China. *Roy. Soc. Open Sci.* 5 (9), 180612.
- Wang, W., Hu, M., Shu, X., Li, H., Qi, W., Yang, Y., Zhang, Q., 2021. Microbiome of permeable sandy substrate in headwater river is shaped by water chemistry rather than grain size and heterogeneity. *Sci. Total Environ.* 780, 146552.
- Wang, X., Kong, F., Li, Y., Li, Q., Wang, C., Zhang, J., Xi, M., 2021. Effect of simulated tidal cycle on DOM, nitrogen and phosphorus release from sediment in Dagu River-Jiaozhou Bay estuary. *Sci. Total Environ.* 783, 147158.
- Wiegner, T.N., Mead, L.H., Molloy, S.L., 2013. A comparison of water quality between low- and high-flow river conditions in a tropical estuary, Hilo Bay, Hawaii. *Estuar. Coast.* 36 (2), 319–333.
- Worrall, F., Burt, T.P., Howden, N.J.K., Whelan, M.J., 2012. The fluvial flux of nitrate from the UK terrestrial biosphere – an estimate of national-scale in-stream nitrate loss using an export coefficient model. *J. Hydrol.* 414–415, 31–39.
- Wu, Y., Wang, X., Wang, H., 2015. Adsorption kinetics of nitrate nitrogen in surface sediments of Yellow River from Inner Mongolia (in China). *Environ. Sci. Technol.* 38 (08), 279–284.
- Wu, F., Wang, Y., Xia, C., Huo, J., Wei, B., 2016. Sorption of ammonia nitrogen on suspended sediments in Lanzhou section of the Yellow River, China. *Fresen. Environ. Bull.* 25, 4–13.
- Xia, X., Liu, T., Yang, Z., Michalski, G., Liu, S., Jia, Z., Zhang, S., 2017. Enhanced nitrogen loss from rivers through coupled nitrification-denitrification caused by suspended sediment. *Sci. Total Environ.* 579, 47–59.
- Xu, N., Tan, G., Wang, H., Gai, X., 2016. Effect of biochar additions to soil on nitrogen leaching, microbial biomass and bacterial community structure. *Eur. J. Soil Biol.* 74, 1–8.
- Yang, H., Zhang, G., Yang, X., Wu, F., Zhao, W., Zhang, H., Zhang, X., 2017. Microbial community structure and diversity in cellar water by 16S rRNA high-throughput sequencing. *Environ. Sci.* 38 (4), 1704–1716.
- Yang, N., Zhang, C., Wang, L., Li, Y., Zhang, W., Niu, L., Zhang, H., Wang, L., 2021. Nitrogen cycling processes and the role of multi-trophic microbiota in dam-induced river-reservoir systems. *Water Res.* 206, 117730.
- Yu, R., Zhang, C., 2021. Early warning of water quality degradation: a copula-based Bayesian network model for highly efficient water quality risk assessment. *J. Environ. Manag.* 292, 112749.
- Yu, Z., Baoqing, S., Wenzhong, T., Hong, Z., 2015. Nitrogen mineralization and geochemical characteristics of amino acids in surface sediments of a typical polluted area in the Haihe River Basin, China. *Environ. Sci. Pollut. Res.* 22 (22), 17975–17986.
- Yu, Z., Zhong, X., Yu, C., Wang, C., Duan, P., Wen, L., You, Y., 2017. Characteristics of nutrient release from sediments under different flow conditions. *Chem. Spec. Bioavail.* 29 (1), 70–77.
- Zhang, B., Chen, D., 2014. Dynamic response of riverine nitrate flux to net anthropogenic nitrogen inputs in a typical river in Zhejiang Province over the 1980–2010 period (in China). *Environ. Sci.* 35 (08), 2911–2919.
- Zhang, S., Xia, X., Yu, L., Zhang, Z., Wang, J., Wang, A., Wang, G., 2020. Both microbial abundance and community composition mattered for N₂ production rates of the overlying water in one high-elevation river. *Environ. Res.* 189, 109933.
- Zheng, X., Zhang, S., Huang, D., Zhang, L., Zhang, J., 2019. A pilot-scale deep bed denitrification filter for secondary effluent treatment using sodium acetate as external carbon. *Water Environ. Res.* 91 (4), 491–499.
- Zhong, X., Wang, C., Yu, C., Wen, L., Duan, P., 2017. Characteristics of sediment sand nutrient release under different flow velocity. *Acta Sci. Circumst.* 37 (08), 2862–2869.
- Zhu, Y., Jin, X., Tang, W., Meng, X., Shan, B., 2019. Comprehensive analysis of nitrogen distributions and ammonia nitrogen release fluxes in the sediments of Baiyangdian Lake, China. *J. Environ. Sci.* 76, 319–328.